

THE USE OF DUAL BOUNDARY ELEMENT METHOD IN THE DYNAMIC ANALYSIS OF STIFFENED PLATES

Sandro Petry Laureano Leme - Centro Universitário Anhanguera de Campo Grande

Francisco Cristóvão Lourenço de Melo, Maria Lourenço de Melo - Universidade de São Paulo - USP

ABSTRACT: In this paper is presented the use of Dual Boundary Element Method (DBEM) in the Laplace transform domain to analyse the dynamic response of stiffened plates of 2 D problems. The formulation is derived by coupling dynamic boundary element two-dimensional plane stress or strain dynamic elasticity formulation of a stiffened plate and the displacement equations for an isolated beam under dynamic load. The interaction forces between stiffeners and the plate are treated as line distributed body forces along the attachment.

PALAVRAS-CHAVE:

banco de dados; auditoria; regras; segurança

KEYWORDS:

dual boundary elements, stiffeners

Artigo Original

Recebido em: 30/10/2009

Avaliado em: 15/07/2013

Publicado em: 22/04/2014

Publicação

Anhanguera Educacional Ltda.

Coordenação

**Instituto de Pesquisas Aplicadas e
Desenvolvimento Educacional - IPADE**

Correspondência

Sistema Anhanguera de

Revistas Eletrônicas - SARE

rc.ipade@anhanguera.com

1. INTRODUCTION

Thin plate structures are widely used in analysing engineering structures (Wen et al., 2000). The dynamic analysis is sometimes more precisely than the static one and for some cases must be employed rather than the static analysis. The applications of boundary element method to the dynamic analysis for plate bending problem were presented by Bezin (1991). A comprehensive description of recent advances in BEM in plate bending can be found in Ref. (Aliabadi, 1998).

The application of the dynamic equations to isolate beams together with the DBEM in the Laplace Domain allow us to evaluate the behaviour of stiffened structure when they are subjected a dynamic loads. This paper intends to show the first results of the use of the Dual Boundary Element Method with dynamic loads in stiffened plates.

First it will be derived the equations to the lateral and longitudinal vibration of an isolated beam under an external harmonic load. Then with the use of some compatibility consideration it will be developed the equations of motions of the internal points of the plate with the presence of the stiffener.

Mathematical Equations for the Vibrating isolated Beam

Considering a stiffener plate as shown in figure 1(a) reinforced with stiffeners in the both side of the plate. This type of construction allows us to consider the problem in 2 dimensions because of the symmetric construction which minimize the effects of the out of plane displacements. Also the loads are only in the direction x or y given thus only the 2D analysis of the problem, the considering forces in plate and the forces and momentums in the stiffeners are showed in figure 1(b).

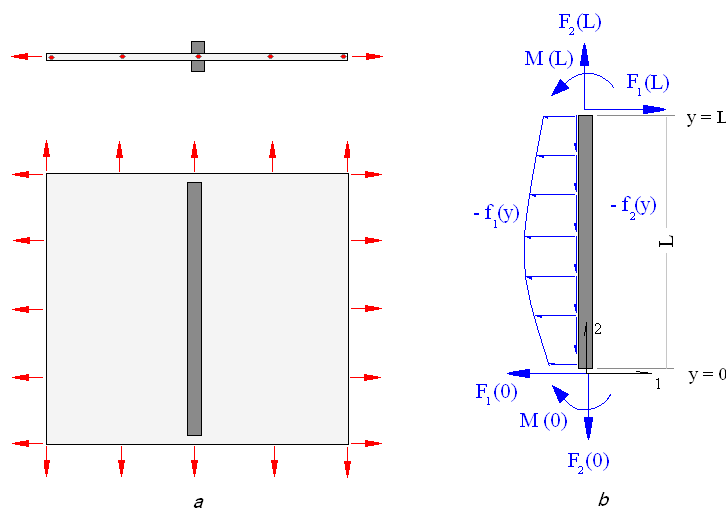


Figure 1 – (a) Stiffened plate; (b) Forces and Momentums applied over the stiffener.

For the lateral direction (over the axe 1 in the figure) the differential equation of motion takes the form:

$$EJ \frac{\partial^4 u(y,t)}{\partial x^4} + \rho \frac{\partial^2 u(y,t)}{\partial t^2} = p(y,t) \quad (1)$$

If the load is harmonic

$$p(y,t) = p(y) \sin \omega t \quad (2)$$

where
$$p(y) = F_1(0) - F_1(L) + f_1(y) \quad (3)$$

Substituting eqs. (2) and (3) in eq. (1) and doing some simple rearrangement we get the following equation (Kolousek, 1973).

$$EJ \frac{d^4 u(y)}{dy^4} + \rho \omega^2 u(y) = p(y) \quad (4)$$

The general response, considering $p(x) = 0$ for the equation above is the following:

$$u(y) = A \cos \lambda y/l + B \sin \lambda y/l + C \cosh \lambda y/l + D \sinh \lambda y/l \quad (5)$$

with

$$\lambda = l \left(\frac{\rho \omega^2}{EJ} \right)^{1/4} \quad (6)$$

It must be consider also the particular solution for the equation (1), when it is considered the value of $p(y)$.

The integration constants are computed from the boundary conditions. In this case we consider an arbitrary rotation and displacement at the beginning and end of the beam. For our case we can use the following relations (Meriam and Kraige,1992):

$$-\frac{M(y)}{EJ} = u''(y) \quad (7)$$

and

$$-\frac{T(y)}{EJ} = u'''(y) \quad (8)$$

and from eq. (5) considering that the answer inside the stiffener has a linear variation,

then the second and third derivatives are:

$$u''(y) = \frac{\lambda^2}{l^2} \left(-A \cos \frac{\lambda y}{l} - B \sin \frac{\lambda y}{l} + C \cosh \frac{\lambda y}{l} + D \sinh \frac{\lambda y}{l} \right) \quad (9)$$

and

$$u'''(y) = \frac{\lambda^3}{l^3} \left(A \sin \frac{\lambda y}{l} - B \cos \frac{\lambda y}{l} + C \sinh \frac{\lambda y}{l} + D \cosh \frac{\lambda y}{l} \right) \quad (10)$$

So using the conditions for the beginning and the end of the stiffener $y = 0$ and $y = L$ respectively we have:

$$A = \frac{M(0) l^2}{EJ \lambda^2} + C \quad (11)$$

$$B = \frac{F_1(0) l^3}{EJ \lambda^3} + D \quad (12)$$

$$C = \left[\frac{M(L) l^2}{EJ \lambda^2} - \frac{F_1(0) l^3}{EJ \lambda^3} \sin \lambda - \frac{M(0) l^2}{EJ \lambda^2} \cos \lambda \right] \frac{1}{\cos \lambda - \cosh \lambda} - D \frac{\sin \lambda - \sinh \lambda}{\cos \lambda - \cosh \lambda}$$

$$D = \left[\frac{M(L) l^2}{EJ \lambda^2} - \frac{F_1(0) l^3}{EJ \lambda^3} \sin \lambda - \frac{M(0) l^2}{EJ \lambda^2} \cos \lambda \right] \frac{(-\sin \lambda - \sinh \lambda)}{2(\cos \lambda \cosh \lambda - 1)} + \quad (13)$$

$$\left[\frac{F_1(0) l^3}{EJ \lambda^3} - \frac{M(0) l^2}{EJ \lambda^2} \sin \lambda - \frac{F_1(L) l^3}{EJ \lambda^3} \right] \frac{(\cos \lambda - \cosh \lambda)}{2(\cos \lambda \cosh \lambda - 1)} \quad (14)$$

For the longitudinal direction the differential equation takes the form.

$$ES \frac{\partial^2 v(y,t)}{\partial x^2} - \rho \frac{\partial^2 v(y,t)}{\partial t^2} - p(y,t) = 0 \quad (15)$$

If the load is harmonic

$$p(y,t) = p(y) \sin \omega t \quad (16)$$

where
$$p(y) = F_2(0) - F_2(L) + f_2(y) \quad (17)$$

Substituting eqs. (13) and (14) in eq. (12) and doing some simple rearrangement we get the following equation (Kolousek, 1973).

$$ES \frac{d^2 v(y)}{dy^2} + \rho \omega^2 v(y) = p(y) \quad (18)$$

The general response for the equation above is the following

$$v(x) = G \cos \psi y/l + H \sin \psi y/l \quad (19)$$

with

$$\psi = l \left(\frac{\rho \omega^2}{ES} \right)^{1/2} \quad (20)$$

The same procedure must be taken to determine the particular solution of the equation (12). The integration constants are also computed from the boundary conditions. For the case here we have the following relation:

$$\frac{N(y)}{ES} = v'(y) \quad (21)$$

and from eq. (19) the first derivative is:

$$v'(y) = \frac{\psi}{l} \left(-E \sin \psi y/l + F \cos \psi y/l \right) \quad (22)$$

So using the conditions for the beginning and the end of the stiffener $y = 0$ and $y = L$ respectively we have:

$$G = H \frac{\cos \psi}{\sin \psi} - \frac{F_2(L)}{ES} \frac{l}{\psi} \frac{1}{\sin \psi} \quad (23)$$

$$H = \frac{F_2(0)}{ES} \frac{l}{\psi} \quad (24)$$

2. DUAL BOUNDARY ELEMENT METHOD

The general field equation for elastodynamics, may be written as (Domingues, 1993):

$$c_1^2 \nabla \nabla u - c_2^2 \nabla x \nabla x u - \frac{\partial^2 u}{\partial t^2} = -b \quad (25)$$

where $c_1 = (\lambda + 2\mu/\rho)^{1/2}$ is the P-wave velocity; $c_2 = (\mu/\rho)^{1/2}$ is the S-wave velocity; λ and μ are the Lamé constants; ρ is the density; and ρb is the body force vector and u is the displacement vector.

For 2 D dynamic problems the fundamental solutions are:

$$U_{ij} = \frac{1}{2\pi\rho c_2^2} [\psi \delta_{ik} - \chi r_{,l} r_{,k}] \tag{26}$$

$$T_{ij} = \frac{1}{2\pi} \left[\left(\frac{d\psi}{dr} - \frac{1}{r} \chi \right) \left(\delta_{ik} \frac{\partial r}{\partial n} + r_{,k} n_{,l} \right) - \frac{2}{r} \chi \left(n_{,k} r_{,l} - 2r_{,l} r_{,k} \frac{\partial r}{\partial n} \right) - 2 \frac{d\chi}{dr} r_{,l} r_{,k} \frac{\partial r}{\partial n} + \dots \right. \\ \left. \dots + \left(\frac{c_1^2}{c_2^2} - 2 \right) \left(\frac{d\psi}{dr} - \frac{d\chi}{dr} - \frac{1}{r} \chi \right) r_{,l} n_{,k} \right] \tag{27}$$

The value for the functions Ψ and χ for the 2D analysis are given in the appendix.

The Dual Boundary Element Method (DBEM), as presented by Portela et al. (Portela et al, 1992), is capable of analysing configurations involving any number of edges and embedded cracks in any given geometry. The need for dividing the problem in different regions, common to many boundary element formulations, is avoided by using the displacement equation when collocating at one crack surface and the dual traction equation when collocating at the other crack surface (Salgado et al., 1996). The use of Laplace Transform enables us to have a simpler way to analyse the problem and to achieve reasonable answers for dynamic analysis.

The boundary integral displacement equation, for a source point x' at the boundary Γ of a finite sheet is give by:

$$c_{ij}(x') u_j(x') + \int_{\Gamma} T_{ij}(x', x) u_j(x) d\Gamma(x) = \int_{\Gamma} U_{ij}(x', x) t_j(x) d\Gamma(x) \dots \\ \dots + \iint_{\Omega} U_{ij}(x', X) b_j(X) d\Omega(X) \tag{28}$$

where $T_{ij}(x', x)$ and $U_{ij}(x', x)$ are the Kelvin traction and displacement fundamental solutions, respectively, $u_j(x)$ and $t_j(x)$ are the displacements and tractions at boundary field points x , $b_j(X)$ are body forces acting at field points X inside the domain Ω and c_{ij} is a coefficient that can be determined by rigid body movement considerations.

The corresponding traction boundary integral equation, presented below, can be obtained by differentiation of equation (28), application of the Hooke's law and multiplication by the outward normal,

$$\frac{1}{2} t_j(x') + n_i(x') \int_{\Gamma} S_{ijk}(x', x) u_k(x) d\Gamma(x) = n_i(x') \int_{\Gamma} D_{ijk}(x', x) t_k(x) d\Gamma(x) \dots \\ \dots + n_i(x') \iint_{\Omega} D_{ijk}(x', X) b_k(X) d\Omega(X) \tag{29}$$

where $S_{ijk}(x', x)$ and $D_{ijk}(x', x)$ contain derivatives of $T_{ij}(x', x)$ and $U_{ij}(x', x)$, respectively and $n_i(x')$ denotes the i -th component of the unit outward normal to the boundary at the source point x' . The plate is considered to be thin, so that the interactions forces exchanged with the stiffeners can be treated as action-reaction body forces. The plate displacement and traction equations can be derived by considering equations (28) and (29) which assume the presence

of body forces. If, instead of being distributed over the whole domain, the body forces are confined to straight lines inside it, the domain integrals in equations (28) and (29) reduce to line integrals over the body forces loci. The displacement and traction equations for a thin plate with N stiffeners continuously bonded to it can thus be written as:

$$c_{ij}(x') u_j(x') + \int_{\Gamma} T_{ij}(x', x) u_j(x) d\Gamma(x) = \int_{\Gamma} U_{ij}(x', x) t_j(x) d\Gamma(x) \dots$$

$$\dots + \frac{1}{h} \sum_{n=1}^N \int_{\Gamma_{Sn}} U_{ij}(x', X) b_j^{Sn}(X) d\Gamma_{Sn}(X) \quad (30)$$

and

$$\frac{1}{2} t_j(x') + n_i(x') \int_{\Gamma} S_{ijk}(x', x) u_k(x) d\Gamma(x) = n_i(x') \int_{\Gamma} D_{ijk}(x', x) t_k(x) d\Gamma(x) \dots$$

$$\dots + n_i(x') \frac{1}{h} \sum_{n=1}^N \int_{\Gamma_{Sn}} D_{ijk}(x', X) b_k^{Sn}(X) d\Gamma_{Sn}(X) \quad (31)$$

where Γ_{Sn} stands for the stiffeners loci, b_k^{Sn} represents the unknown sensor attachment forces and h is the plate thickness.

3. DISPLACEMENT COMPATIBILITY

The displacement compatibility conditions for points at the stiffeners attachment region are based on the assumption that the displacement u_j of a point X' ($X' \in \Gamma_{Sn}$) at the plate and u_j^{Sn} of a corresponding point at the n -th stiffener, has to be compatible with the shear deformation of the adhesive layer connecting the sensor to the plate. They are expressed, with respect to a reference point X^0 at the same sensor locus ($X^0 \in \Gamma_{Sn}^0$), by N sets of relations as:

$$\Delta u_j(X') - \Delta u_j^{Sn}(X') = \frac{h_{Ad}}{G_{Ad}} \Delta \tau_j^{Ad}(X') \quad (32)$$

where h_{Ad} is the thickness of the adhesive layer, G_{Ad} is the coefficient of shear deformation of the adhesive material, τ_j^{Ad} is the shear stress at the adhesive, $\Delta u_j(X') = u_j(X') - u_j(X^0)$, $\Delta u_j^{Sn}(X') = u_j^{Sn}(X') - u_j^{Sn}(X^0)$, $\Delta \tau_j^{Ad}(X') = \tau_j^{Ad}(X') - \tau_j^{Ad}(X^0)$. For the line stiffeners, the adhesive shear stress τ_j^{Ad} are equal in value to the attachment forces b_j^{Sn} divided by the width of the adhesive line w_{Ad} . The displacement compatibility equation can be written in terms of the body forces as:

$$\Delta u_j(X') - \Delta u_j^{Sn}(X') = \Phi_{Ad} \Delta b_j^{Sn}(X') \quad (33)$$

where $\Delta b_j^{Sn}(X') = b_j^{Sn}(X') - b_j^{Sn}(X^0)$ and

$$\Phi_{Ad} = \frac{h_{Ad}}{w_{Ad} G_{Ad}} \quad (34)$$

is the coefficient of shear deformation of the adhesive.

If the reference point X^0 is taken to coincide with the sensor starting point ($y=0$), the relative displacement Δu_j^{Sn} in equation (30) can be expressed as a function of the unknown interaction forces b_j^{Sn} , by using the expression (5) for the transverse displacement and (19) for the longitudinal displacement. The relationship between the relative displacements and forces expressed in terms of the plate and the sensors coordinate systems is given by:

$$\Delta u_i^{Sn} = \Theta_{ij}^{Sn} \Delta v_j^{Sn} \tag{35}$$

and

$$b_i^{Sn} = \Theta_{ij}^{Sn} f_j^{Sn} \tag{36}$$

The transformation matrix being:

$$\Theta^{Sn} = \begin{bmatrix} + \cos \varphi^{Sn} & - \sin \varphi^{Sn} \\ + \sin \varphi^{Sn} & + \cos \varphi^{Sn} \end{bmatrix} \tag{37}$$

where φ^{Sn} is the angle between the plate direction x_2 and the n -th sensor axis.

The plate relative displacement $\Delta u_j(X') = u_j(X') - u_j(X^0)$ in equation (30) can be then finally written as:

$$\begin{aligned} \Delta u_j(X') = & \int_{\Gamma} [U_{ij}(X', x) - U_{ij}(X^0, x)] t_j(x) d\Gamma(x) - \int_{\Gamma} [T_{ij}(X', x) - T_{ij}(X^0, x)] u_j(x) d\Gamma(x) + \dots \\ & \dots + \frac{1}{h} \sum_{n=1}^N \int_{\Gamma_{Sn}} [U_{ij}(X', X) - U_{ij}(X^0, X)] b_j^{Sn}(X) d\Gamma_{Sn}(X) \end{aligned} \tag{38}$$

The problem can be totally solved by making use of the Equilibrium equations over each stiffener.

For the stiffeners to be in equilibrium, the following equations have to be satisfied:

$$F_1(L) - F_1(0) - \int_0^L f_1(y) dy = 0 \tag{39}$$

$$F_2(L) - F_2(0) - \int_0^L f_2(y) dy = 0 \tag{40}$$

$$M(L) - M(0) - LF_1(0) = \int_0^L (L - y) f_1(y) dy \tag{41}$$

4. NUMERICAL EXAMPLES

PLATE WITH ONE STIFFENER

The first numerical example is a plate with one stiffener, using plane stress conditions to solve the problem in 2D. The different positions of the stiffener inside the plate can be seen in the figure 2. Also the boundary conditions are showed in figure 2. For this example were used 12 boundaries elements, the material applied in the plate was steel, also for the stiffeners. The dimensions of the plate are $width = 20\text{ m}$, $high = 40\text{ m}$. Each stiffener has $area = 5\text{ m}^2$. The load applied on the upper part of the plate has unitary amplitude. For maintaining simplicity the concentrate loads and momentums at the ends of each stiffener are here considered zero. The graph of figure 3 shows the result for the three different sets of stiffeners positions. The two curves are the comparison between the static code (Salgado et al., 1996) with the dynamic one when in this last one we took the frequency very low ($\omega = 0.001$).

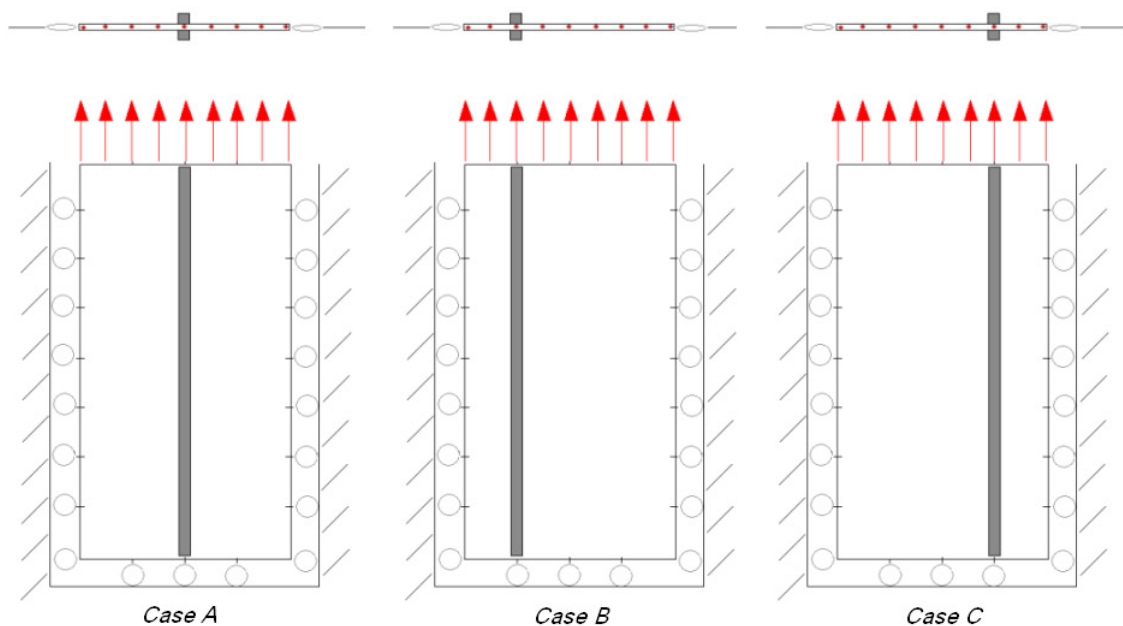


Figure 2 – Mesh and boundaries conditions applied for the plate with one stiffener.

The agreements of the curves are satisfactory considering that was used a very little value to the frequency to get to the static value of the displacement. The y axis of the graph was normalized using the v_0 displacement equals to the displacement of the central node of the upper part of the plate without the use of stiffener (equals to 0.4574 mm). The x axis was normalized with the distance $d = 20.0\text{ m}$ and x varies from 0 to 20.

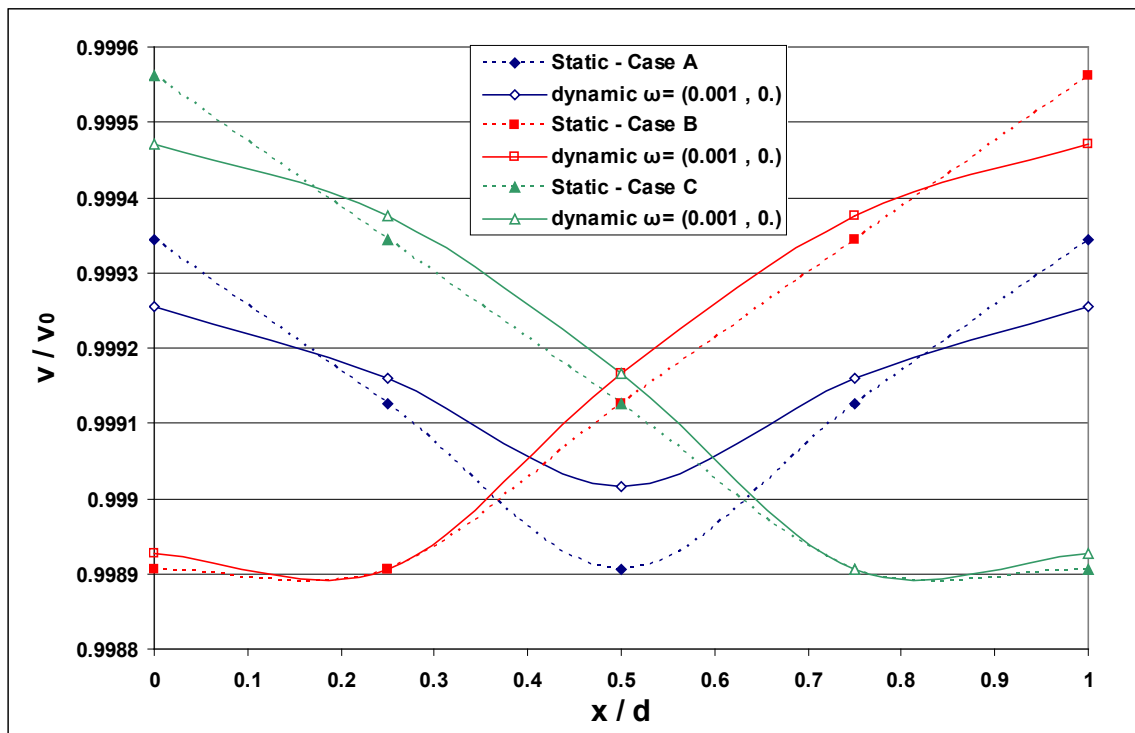


Figure 3 – Displacement values along top edge of the one stiffened plate using static and dynamic codes.

5. PLATE WITH TWO STIFFENERS

The second numerical example is a plate with two stiffeners. The different positions of the stiffener inside the plate can be seen in the figure 4. Also the boundary conditions are showed in figure 4. For this example were used 12 boundaries elements, the material applied in the plate was steel, also for the stiffeners. The dimensions of the plate are *width* = 20 m, *high* = 40 m. Each stiffener has *area* = 5 m². The load applied on the upper part of the plate has unitary amplitude. The graph of figure 5 shows the result for the three different sets of stiffeners positions. The two curves are the comparison between the static code (Salgado et al., 1996) with the dynamic one when in this last one we took the frequency very low ($\omega = 0.001$).

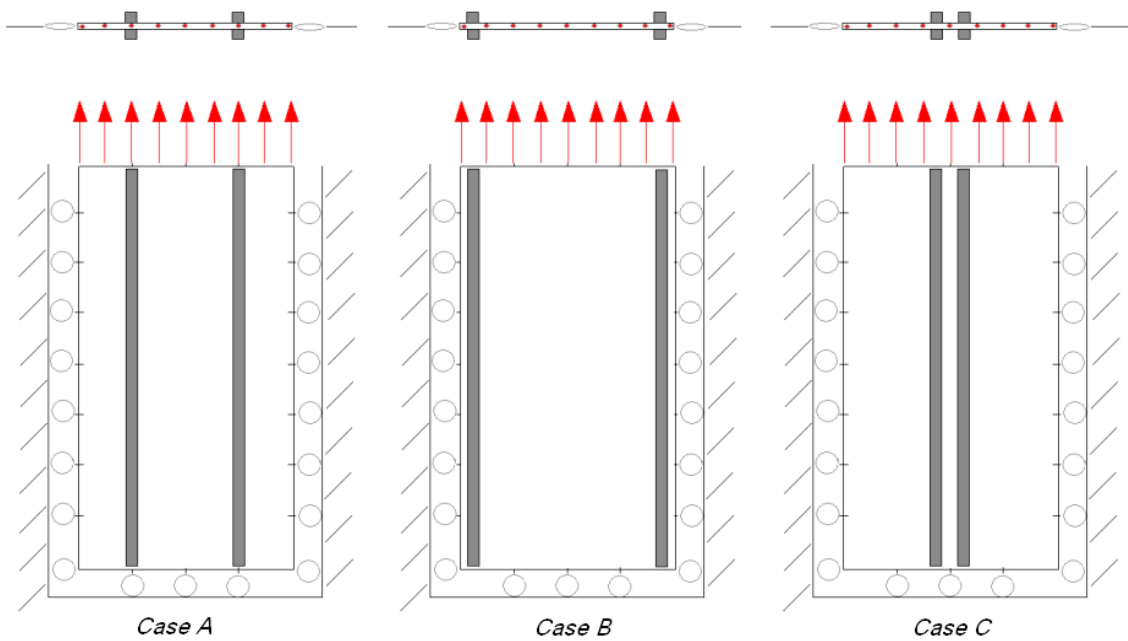


Figure 4 – Mesh and boundaries conditions applied for the plate with two stiffeners.

The agreements of the curves are satisfactory considering that was used a very little value to the frequency to get to the static value of the displacement. The y axis of the graph was normalized using the v_0 displacement equals to the displacement of the central node of the upper part of the plate without the use of stiffener (equals to 0.4574 mm). The x axis was normalized with the distance $d = 20.0 \text{ m}$ and x varies from 0 to 20.

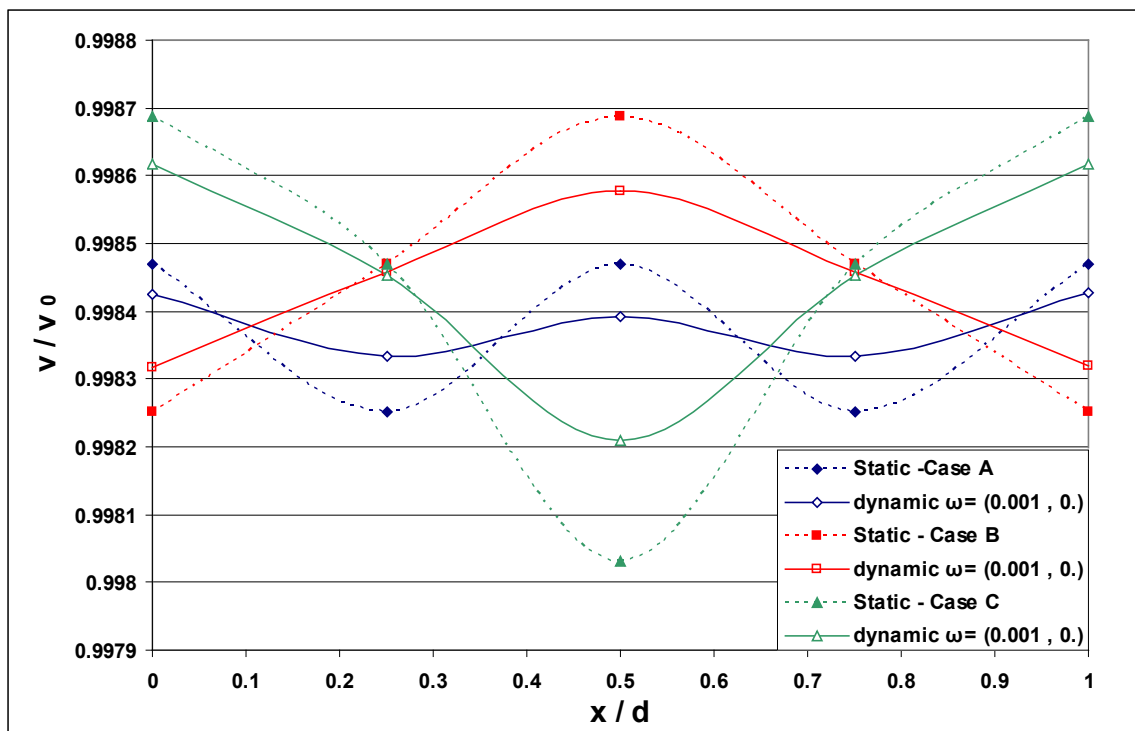


Figure 5 – Displacement values along top edge of the two stiffened plate using static and dynamic codes.

6. PLATE WITH THREE STIFFENERS

The third example is a plate with three stiffeners and the boundaries conditions showed in the figure 6. For this example were used 24 boundaries elements, the material applied in the plate was steel, also for the stiffeners. The dimensions of the plate are $width = 20\ m$, $high = 40\ m$. Each stiffener has $area = 5\ m^2$. The load applied on the upper part of the plate has unitary amplitude. The graph of figure 7 shows the result for the three different sets of stiffeners positions. The first two curves are for the stiffeners positioned like showed in the figure 6. The curves obtained with the code used here are compared with other curves from static codes (Salgado et al., 1996). The other set of curves are for the stiffeners in different position inside the plate. The stiffeners were positioned in the corners of the plate and one in the centre and the last set of curves is for the stiffeners agglomerate more in the centre of the plate.

The agreements of the curves are satisfactory considering that was used a very little value to the frequency to get to the static value of the displacement. The y axis of the graph was normalized using the v_0 displacement equals to the displacement of the central node of the upper part of the plate without the use of stiffener (equals to $0.4574\ mm$). The x axis was normalized with the distance $d = 20.0\ m$ and x varies from 0 to 20.

Figure 6 – Mesh and boundaries conditions applied for the plate with three stiffeners.

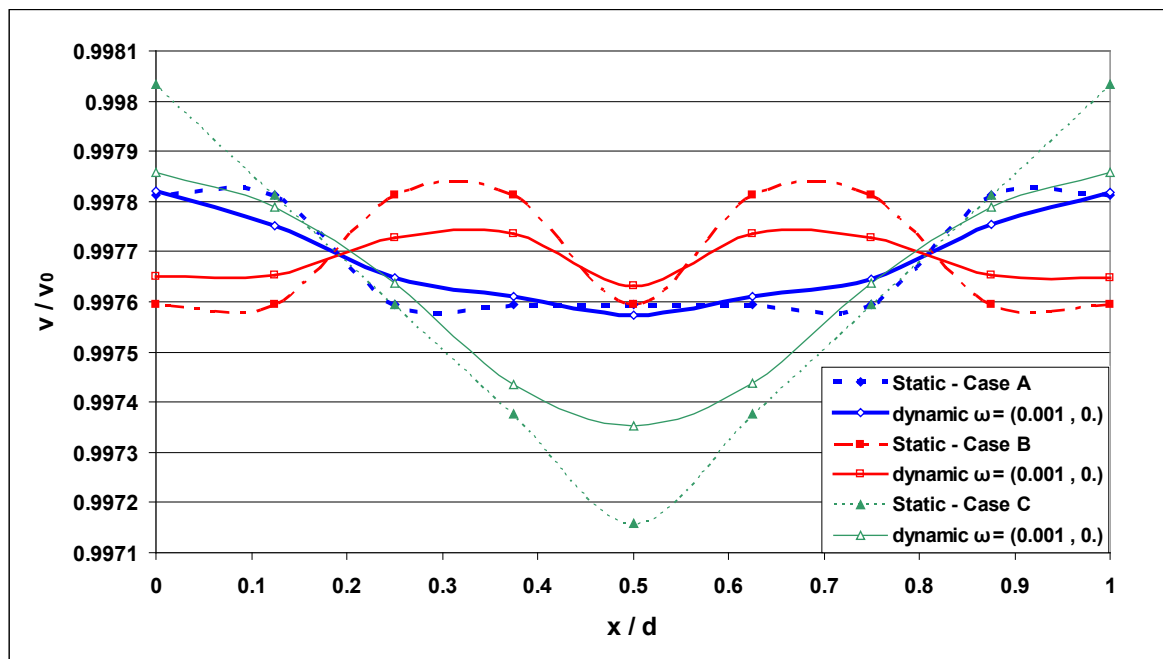


Figure 7 – Displacement values along top edge of the three stiffened plate using static and dynamic codes.

6.1. Stress Intensive Factor (SIF) for the Plate with two Stiffeners – slant crack

In this next numerical example, now we compute the values of the Stress Intensity Factors (SIF) K_I and K_{II} normalized by the value of K_{I0} , which is the value for the SIF for the same static problem. The configuration of the plate is showed in figure 8 and the results are showed in figure 9. Here the plate has the following dimensions: 3 m width and 6 m high. The crack is slant and the values of the SIFs are computed for a different relation $d/2a$ and compared with the values of the SIF for the plate without stiffeners. The figure 9 shows the results for this problem.

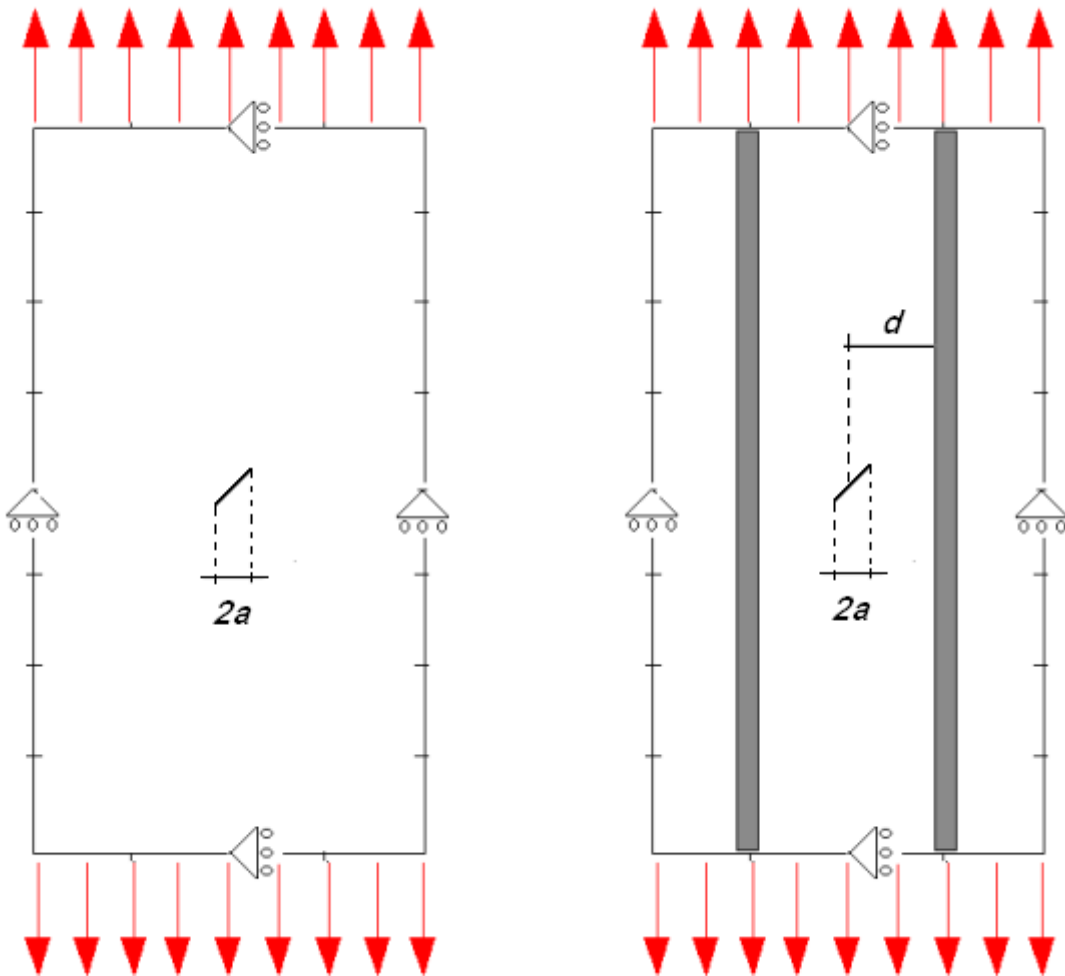


Figure 8 – Plate used for the SIFs (K_I and K_{II}) calculations.

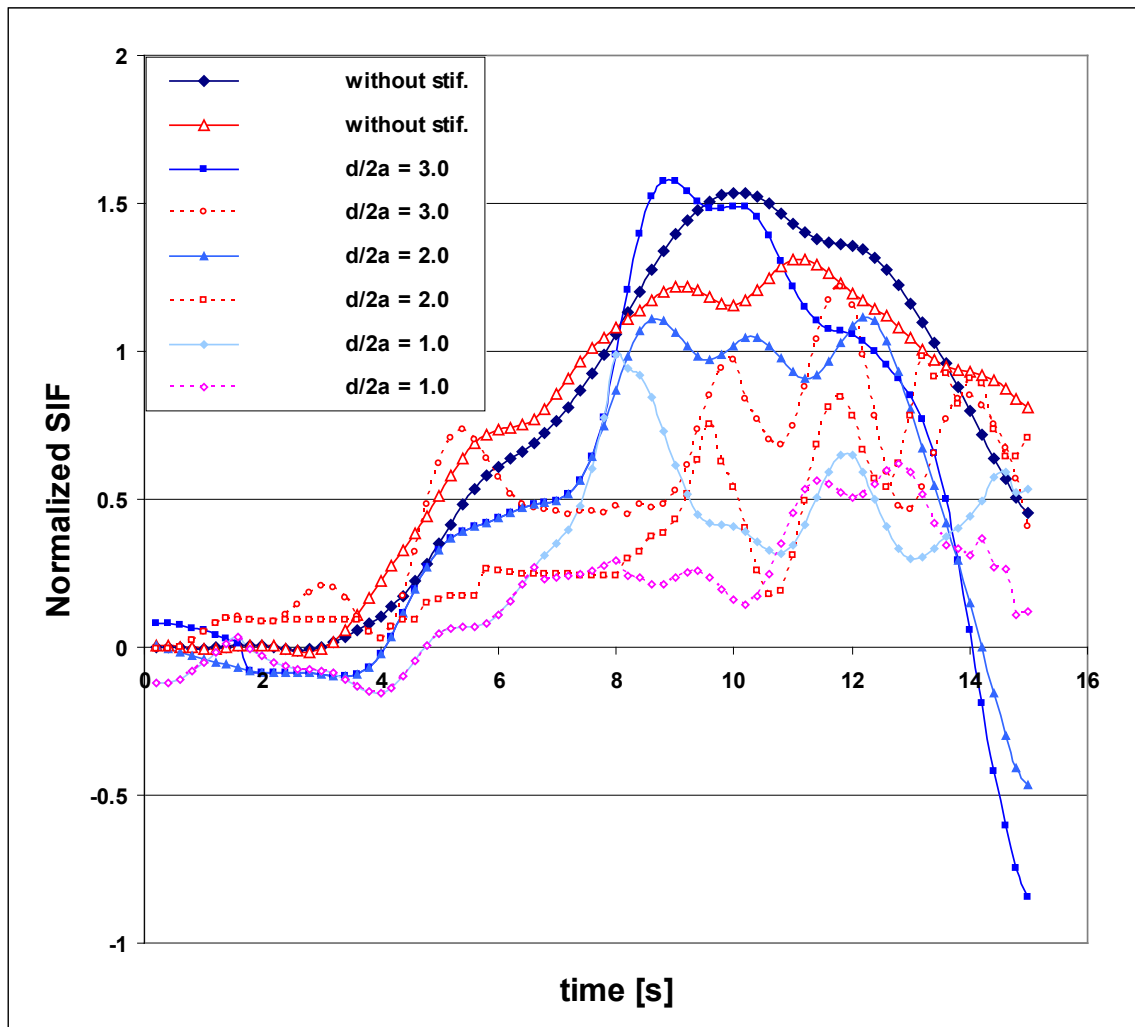


Figure 9 – Values of the Normalized SIF for different values of $d/2a$.

6.2. Stress Intensive Factor (SIF) for the Plate with two Stiffeners – straight crack

In this last numerical example, now we compute the values of the Stress Intensity Factors (SIF) K_I for the plate showed in figure 10. The crack is straight and the values of the SIF are computed for a different relation $d/2a$ and compared with the values of the SIF for the plate without stiffeners. The figure 11 shows the results for this problem.

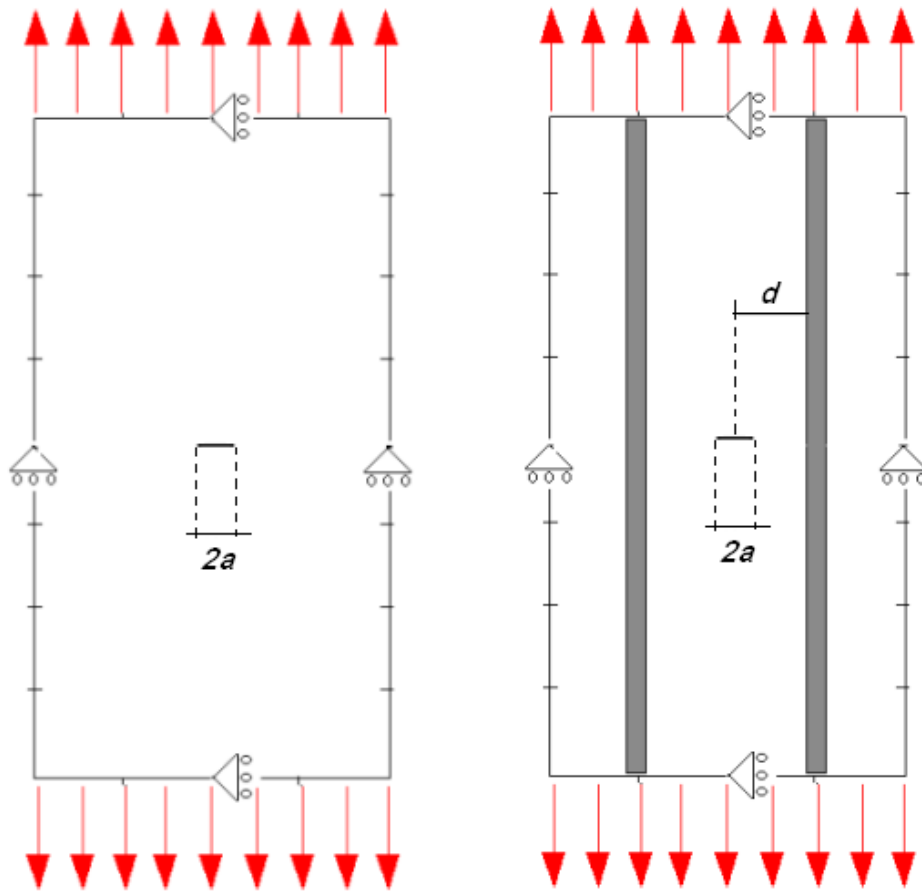


Figure 10 – Plate used for the SIF (K_I) calculations.

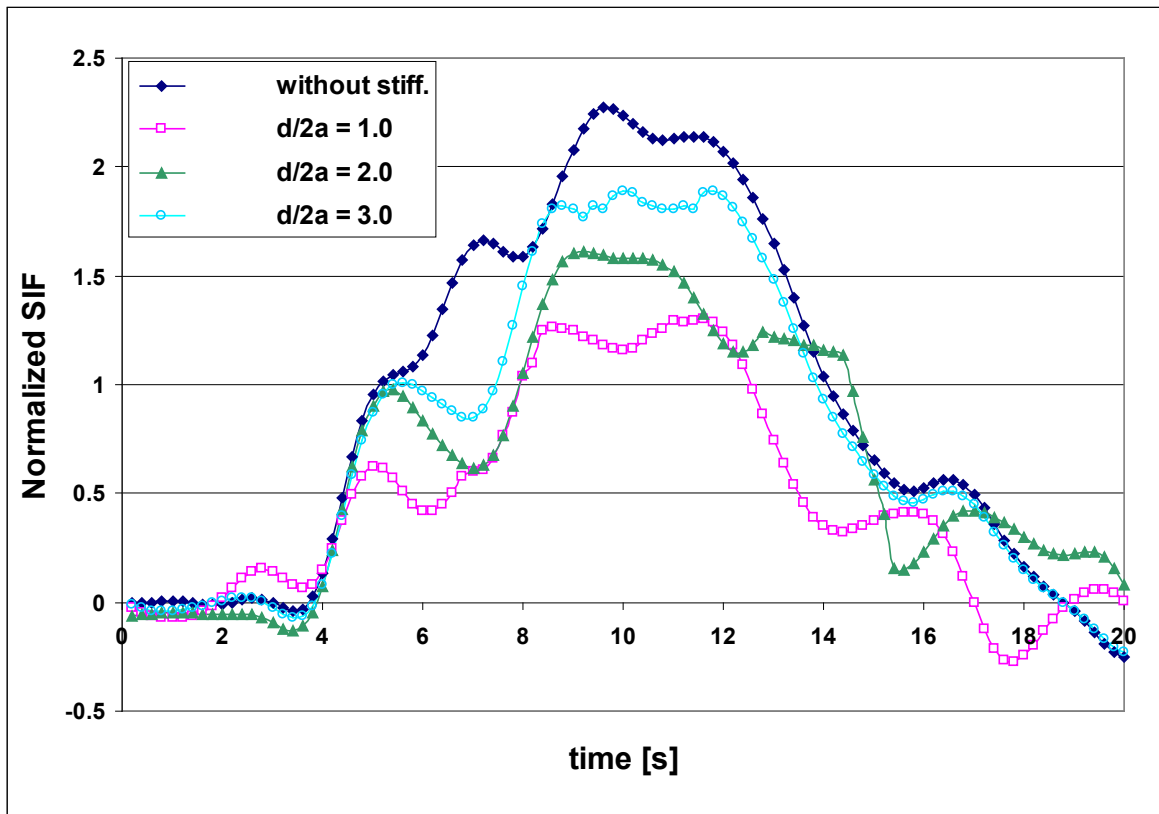


Figure 11 – Values of the Normalized SIF for different values of $d/2a$.

7. CONCLUSIONS

The use of the code in dynamic for the plate with the stiffeners could represent some advantage in the analysis of the stress intensity factors because the real problems in the majority of the structures are really occurring during the use and over dynamics loads. The improvement of such codes can improve the analysis of critical structures and allow more confidence in the analysis.

8. ACKNOWLEDGEMENTS

The authors gratefully acknowledge CNPq (Brazilian National Research Council) and CAPES Foundation (Foundation for the Coordination of Higher Education and Graduate Training) for their support for this research. And also Dr. P.H. Wen from Queen Mary University for the substantial helps on dynamics aspects.

REFERENCES

- Aliabadi, M.H., 1998. **"Plate Bending Analysis with Boundary Elements."** Computational Mechanics Publications, Southampton UK, Boston USA.
- Aliabadi, M. H. and Rooke, D. P., 1991 **"Numerical Fracture Mechanics"** Solid Mechanics and its Applications, Computational Mechanics Publications.
- Bezin, G., 1991. **"A boundary integral equation method for plane flexure with conditions inside the domain."** Int. J. Numer. Methods Engng. 17, 1467-1657.
- Domingues, J., 1993. **"Boundary Elements in Dynamics"** Computational Mechanics Publications - Southampton - Boston USA.
- Kolousek, V., **"Dynamics in Engineering Structures"** Butterworths, London UK, 1973.
- Leme S.P.L., Aliabadi M.H., Bezerra L.M., Partridge P. W., **"An Investigation into Active Strain Transfer Analysis in a Piezoceramic Sensor System for Structural Health Monitoring Using the Dual Boundary Element Method "** Structural Durability & Health monitoring, vol.3, no.3, pp.121-132, 2007.
- Meriam, J. L., Kraige L.G., **"Engineering Mechanics - Volume two"** John Wiley & Sons, Inc., New York USA, 1992.
- Portela A., Aliabadi M.H. and Rooke, D.P., 1992. **"Dual boundary Element Method, effective implementation for crack problems"** International Journal of Numerical Methods in Engineering, 33, 1269 - 1287.
- Salgado, N. K. and Aliabadi M. H., 1996. **"The application of the Dual Boundary Element Method to the analysis of cracked stiffened panels"** Engineering Fracture Mechanics, 54,

1, 91 – 105.

Wen, P. H., Aliabadi M. H. and Young A., 2000. “**Stiffened cracked plates analysis by dual boundary element method**” *International Journal of Fracture*, 106, 245 – 258.

APENDIX

$$\psi = K_0(k_2 r) + \frac{1}{k_2 r} \left[K_1(k_2 r) - \frac{c_2}{c_1} K_1(k_1 r) \right]$$

$$\chi = K_2(k_2 r) - \frac{c_2^2}{c_1^2} K_2(k_1 r)$$